Bioorganic & Medicinal Chemistry 19 (2011) 6581–6586

Contents lists available at SciVerse ScienceDirect

Bioorganic & Medicinal Chemistry

journal homepage: www.elsevier.com/locate/bmc

Daedalols A–C, fungal-derived BACE1 inhibitors

Analia Sorribas [a], Jorge I. Jiménez [b], Wesley Y. Yoshida [a], Philip G. Williams [a,*]

[a] Department of Chemistry, University of Hawai'i at Manoa, Honolulu, HI 96822, United States
[b] AgraQuest, Inc., 1540 Drew Avenue, Davis, CA 95618, United States

ARTICLE INFO

Article history:
Available online 22 September 2011

Keywords:
Fungal steroids
Daedalol A
Daedalol B
Daedalol C
Daedalea sp.
Payne rearrangement

ABSTRACT

Bioassay-guided fractionation of an extract prepared from the fruiting bodies of a *Daedalea* sp. has led to the isolation of daedalols A–C (**1–3**). The structures of these new triterpenes were elucidated based on extensive NMR spectroscopic and mass spectrometric measurements. Assignment of the relative configuration of **3** required the preparation of a suitable derivative via a Payne rearrangement. The aspartic protease BACE1, an Alzheimer's drug target, was inhibited by **3** with an IC_{50} value of 14.2 μM.

1. Introduction

While there are medications currently used to relieve the symptoms of Alzheimer's disease (AD), drugs that can slow or prevent the onset of AD still have not been developed.[1] The aspartic protease β-secretase (BACE1, memapsin-2) is crucial for the formation of β-amyloid oligomers and insoluble plaques in the brains of patients with Alzheimer's disease (AD).[2–4] These β-amyloid oligomers have been implicated in the observed neurodegeneration, and therefore, inhibition of BACE1 represents one possible therapeutic strategy.[1] We recently began screening, using a chemiluminescent enzyme–fragment complementation assay, for natural products that can inhibit BACE1.[5,6] This screening has resulted in the bioassay-guided isolation of three new triterpenes, daedalols A–C (**1–3**), and one known compound (**4**),[7,8] from an extract of a Panamanian *Daedalea* sp. (Polyporaceae). We report here the isolation, characterization, and biological evaluation of these compounds.

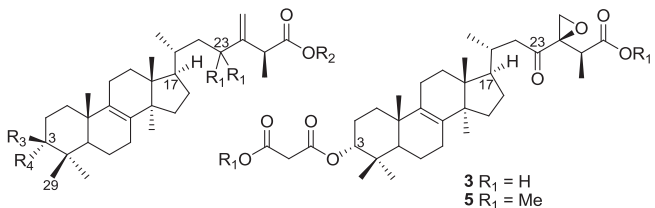

1 R_1 = O R_2 = H R_3 = H R_4 = OH
2 R_1 = H R_2 = H R_3 = R_4 = O
4 R_1 = O R_2 = H R_3 = H R_4 = $O_2CCH_2CO_2H$
6 R_1 = O R_2 = Me R_3 = H R_4 = $O_2CCH_2CO_2Me$

3 R_1 = H
5 R_1 = Me

Exhaustive extraction of the fruiting body sample, followed by orthogonal chromatographic separations led to the isolation of **1** in a yield of 1.7 mg (0.031% yield). Compound **1** generated HR-ESI-TOF (+)-MS $[M+H]^+$ and $[M+Na]^+$ pseudomolecular ions at *m/z* 485.3612 and 507.3418, respectively, corresponding to a molecular formula of $C_{31}H_{48}O_4$. The carbonyl and alkene IR vibrations at 1671 and 1547 cm^{-1}, respectively, explained two of the eight degrees of unsaturation in **1**, implied by the molecular formula. The remaining degrees of unsaturation were rings rather than double bonds due to the lack of any substantial UV absorptions.

Analysis of the proton NMR spectrum of **1** (Table 1) revealed multiple methyl singlets centered around 1.00 ppm that were characteristic of a tetracyclic triterpene. Detailed analyses of the HMBC spectrum provided three substructures consistent with this structural hypothesis (Fig. 1). Fragment C, the most unusual moiety, was assembled based on a COSY correlation between H-20 and H_2-22, and a HMBC correlation from H_2-22 to the carbonyl C-23. HMBC correlations from the terminal alkene protons H_2-24′ to C-23, to a quaternary sp^2 carbon (C-24), and to a methine carbon (C-25), facilitated the construction of the remainder of fragment C.

Fragments A–C were assembled after further analyses of the 2D NMR data. Fragment A was connected to fragment B through HMBC correlations from H_3-19 to C-5, from H_2-7 to C-8, and from H-3 to C-1. A cyclopentane ring was constructed based on a HMBC correlation from H_3-18 of fragment B to C-17 of fragment C, and a COSY correlation between H_2-15 and H_2-16. These assignments completed the final structure as seen in Figure 2.

The spectroscopic data for **2** (3.0 mg, 0.056% yield) was almost identical to that observed for **1**, and thus the two compounds likely had similar structures. A detailed comparison of their NMR spectra

* Corresponding author. Tel.: +1 808 956 5720; fax: +1 808 956 5908.
E-mail address: philipwi@hawaii.edu (P.G. Williams).

0968-0896/$ - see front matter © 2011 Elsevier Ltd. All rights reserved.
doi:10.1016/j.bmc.2011.09.029

Table 1
NMR spectroscopic data (MeOH-d_4) for **1**

	δ_C, mult.	δ_H (J in Hz)[a]	COSY	HMBC[b,c]	ROESY
1	31.3, CH_2	1.45, m	2	3, 5, 19	19
		1.61, m			5
2	26.7, CH_2	1.55, m		3	
		1.93, m	1, 3		19, 29
3	76.6, CH	3.35, dd (2.9, 3.7)	2	5, 28, 29	2, 28, 29
4	38.6, C			3, 6, 28, 29	
5	45.4, CH	1.59, m	6	3, 6, 7, 19	1b, 28
6	19.3, CH_2	1.53, m	5, 7	5, 7	
		1.62, m			
7	27.3, CH_2	2.05, m	6	5, 6	
8	135.2, C			6, 7, 30	
9	136.4, C			5, 7, 19	
10	38.1, C			5, 19	
11	22.0, CH_2	0.94, m	12		
12	32.2, CH_2	1.71, m	11	18	21
		1.78, m			17, 30
13	45.8, C			18, 30	
14	51.2, C			12, 15, 18, 30	
15	31.9, CH_2	1.22, m	16	30	16b, 17, 30
		1.67, m			16a, 18
16	29.4, CH_2	1.36, m	15, 17		
		1.97, m			
17	52.0, CH	1.60, m	16	18, 21, 22	12, 16, 22, 21
18	16.4, CH_3	0.77, s			15b, 19, 20, 21
19	19.5, CH_3	1.02, s			18, 29
20	35.3, CH	2.03, m	21, 22	17, 21, 22	18, 21, 22b
21	20.2, CH_3	0.88, d (6.4)	20	17, 20, 22	17, 20, 18
22	45.7, CH_2	2.52, dd (15.6, 10.1)	20	17, 20, 21	17, 24′b
		2.75, dd (15.6, 2.6)	20		16a, 21
23	203.6, C			22, 25, 24′	
24	150.4, C			25, 27, 24′	
24′	125.9, CH_2	5.94, s		25	25
		6.24, s			22
25	41.9, CH	3.57, q (7.1)	27	27, 24′	27, 24′a
26	179.0, C			25, 27	
27	16.6, CH_3	1.29, d (7.2)	25	25	25
28	28.8, CH_3	0.94, s		3, 29	
29	22.8, CH_3	0.87, s		3, 28	3, 5, 19
30	24.6, CH_3	0.93, s			5, 7, 12b, 15a, 17, 21

[a] Higher field proton designated 'a'.
[b] Optimized for 7 Hz.
[c] Protons showing long-range correlation with indicated carbon.

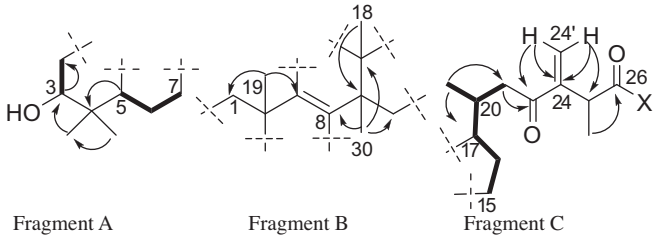

Figure 1. Fragments of **1** assembled using HMBC (H→C) and COSY (▬ bold) correlations.

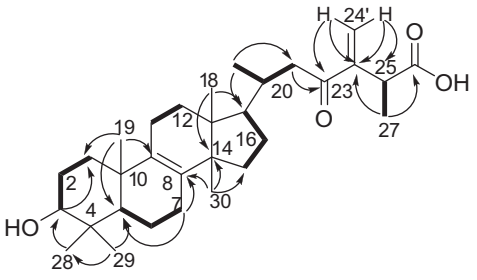

Figure 2. Key HMBC (H→C) and COSY (▬ bold) correlations observed for **1**.

revealed that the resonance for the oxygenated methine H-3 observed in **1** was missing in **2**, and the resonances for H_2-24′ were shifted upfield by more than 1 ppm (Table S1). The carbon NMR spectra reflected these chemical shift differences as well. In the spectrum of **2**, resonances consistent with a ketone at C-3 and an isolated alkene at C-24 were observed. Based on these data, the structure of **2** was proposed as depicted.

Compound **3** was isolated in a yield of 0.033% (1.8 mg). Although the HR-ESI spectrum of **3** indicated a molecular formula of $C_{31}H_{46}O_4$, the ^{13}C NMR spectrum contained 34 resonances. As the NMR data for **3** indicated it was a pure compound, this discrepancy suggested that the observed ion at *m/z* 483 corresponded to a fragment. Therefore, the molecular formula of **3** was established by analyses of the NMR spectroscopic data as $C_{34}H_{50}O_8$, which indicated 10 degrees of unsaturation. On the basis of the observed carbon chemical shifts, five degrees of unsaturation were ascribed to a ketone ($\delta_{C\text{-}23}$ 209.1), an ester ($\delta'_{C\text{-}1}$ 166.9), a single carbon-carbon double bond ($\delta_{C\text{-}9}$ 134.3 and $\delta_{C\text{-}8}$ 133.9), and two carboxyl groups ($\delta_{C\text{-}26}$ 178.9 and $\delta'_{C\text{-}3}$ 171.2).

The tetracyclic core of **3** was assembled through analyses of the 2D NMR data (Table 2). In **3**, the linear side chain (from C-20 to C-26) was converted from the terminal olefin found in **1** and **2**, into an epoxide (Fig. 3). In addition, the downfield shift observed for H-3 in **3**, relative to **1** (**1** $\delta_{H\text{-}3}$ 3.35; **3** $\delta_{H\text{-}3}$ 4.74), indicated that the hydroxyl group at C-3 was esterified with a malonate residue.

Table 2
NMR spectroscopic data (MeOH-d_4) for **3**

	δ_C, mult.	δ_H (J in Hz)[a]	COSY	HMBC[b,c]
1	30.6, CH_2	1.40, m	2	3, 19
		1.47, m		
2	25.8, CH_2	2.05, m	1	3
3	80.4, CH	4.74, m	2	1, 5
4	36.8, C			3, 5, 28, 29
5	45.2, CH	1.43, m	6	3, 19, 28
6	28.5, CH_2	1.22, m	5, 7	
		1.83, m		
7	17.9, CH_2	1.58, m	6	5
		1.45, m		
8	133.9, C			7, 30
9	134.3, C			11, 19
10	38.2, C			1
11	23.1, CH_2	2.09, m	12	12
12	32.1, CH_2	1.68, m		
		1.87, m		
13	44.5, C			18, 30
14	49.9, C			16, 18, 30
15	30.7, CH_2	1.16, m		30
		1.67, m		
16	28.5, CH_2	1.28, m		
		1.93, m		
17	50.1, CH	1.51, m		18, 21, 22
18	15.7, CH_3	0.78, s		
19	18.9, CH_3	0.98, s		1
20	32.9, CH	1.99, m	17, 21, 22	21, 22
21	19.7, CH_3	0.87, s	20	22
22	41.5, CH_2	2.35, dd (17.1, 10.0)		21
		2.16, dd (17.1, 2.9)		
23	209.1, C			22, 25, 24′
24	61.9, C			25, 27, 24′
24′	48.5, CH_2	3.03, d (4.0)		25
		2.99, d (4.0)		
25	41.0, CH	2.86, q (7.4)	27	27, 24′
26	178.9, C			25, 27
27	12.8, CH_3	1.28, d (7.4)	25	25
28	27.0, CH_3	0.92, s		29
29	21.7, CH_3	0.87, s		3, 28
30	24.2, CH_3	0.90, s		
1′	166.9, C			3
2′	40.9, CH_2	3.45, s		
3′	171.2, C			

[a] Higher field proton designated ‘a’.
[b] Optimized for 7 Hz.
[c] Protons showing long-range correlation with indicated carbon.

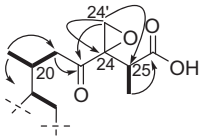

Fragment D

Figure 3. HMBC (H→C) and COSY (▬ bold) correlations used to deduce C-20 through C-27 of **3**.

With a planar structure for **3** assigned, the fragment ion observed at m/z 483.3500 in the MS data could be easily explained. Under the MS analysis conditions, a facile McLafferty rearrangement cleaves off the malonate ester while oxidizing the adjacent ring. Protonation of the resulting tetracyclic fragment yields the $[M+H]^+$ ion observed under positive mode ESI at m/z 483 (Fig. 4).

In addition to **1**–**3**, the known metabolite **4** was isolated from the crude extract. As previously reported,[7] purification of **4** proved difficult due to its poor chromatographic behavior. Instead, a portion of the crude extract, that had been held in reserve, was derivatized with $TMSCHN_2$[9,10] to produce **6**,[7] the known dimethyl ester of **4**. Purification of this derivatized crude extract by normal-phase HPLC yielded the desired compound **6** (30.2 mg), along with 35.7 mg of the dimethyl ester of **3**. Comparison of the NMR spectroscopic data for our sample of **6** (*Tables* S2 and S3) with the revised chemical shift assignments,[8] conclusively established its identity.

The conclusive identification of **6**, whose configuration was previously secured through X-ray crystallography,[7] enabled the relative configurations of **1–3** to be proposed based on biogenetic considerations. These assignments include the configurations of C-20 and C-25 in the linear side chains of **1–3**. Further confirmation of the configuration of the tetracyclic cores in **1**–**3** was obtained through analyses of the ROESY and coupling constant data (Fig. 5). The H-3 methine proton in **1** was equatorial based on the magnitude of the vicinal couplings (2.9, 3.7 Hz) to H_2-2. ROESY correlations from H-3 to H_3-29, H_3-29 to H_3-19, and H_3-19 to H_3-18 defined axial orientations for H_3-18 and H_3-19 as shown in Figure 5. An α-orientation was assigned to H-17 and H_3-30 based on ROESY correlations observed from H_3-30 to H-12b and from H-12b to H-17. All of these data are consistent with the proposed configurations of **1**–**3**.

Only the relative configuration of C-24 in **3** remained to be deduced. Several strategies were considered to solve this problem. Since attempts to crystallize **3** or **5** proved unsuccessful, we opted for a NMR-based strategy. Lacking a reliable method to relate the configurations of C-25 or C-20 to the quaternary center C-24 in **3**, we sought to convert **3**, via **5**, to **8**, reasoning that the configuration of the methine H-23 could be easily related to H-20 in the latter derivative. A key requirement for this process was that the configuration of C-24 be controlled throughout the reaction sequence in a predictable manner.

A Payne rearrangement[11,12] is a stereoselective 1,2-epoxide migration that could convert a terminal epoxide, such as **7**, to the trisubstituted epoxide **8**. Stereoelectronic requirements dictate that the conformation of the transition state for the conversion of **7**–**8** must have the C_{23}–OH σ-bond *anti* to the C_{24}–O antibonding σ^* orbital of the epoxide. This S_N2 reaction would invert the configuration at C-24 in **8** relative to **7**. Assuming the configuration of **8** can be deduced with confidence, it should be a simple matter to relate that back to **7** and therefore, to **3**.

Compound **7** could be produced from **3**, or the dimethyl derivative **5**, via simple reduction. The reduction of **5** has the potential to produce a mixture of diastereomers at C-23. Assuming a single diastereomer of **7** was used as the substrate for the Payne

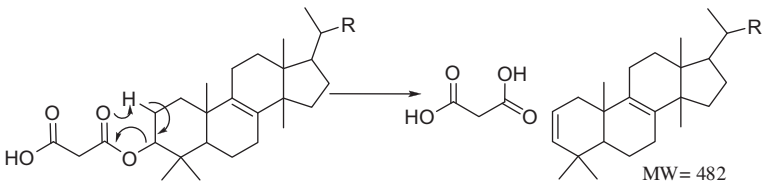

Figure 4. McLafferty rearrangement of **3** observed under ESI-MS analysis.

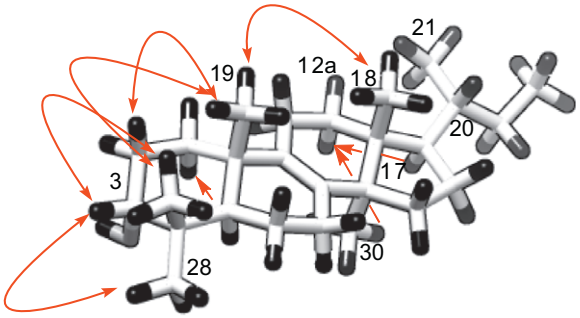

Figure 5. Key ROESY correlations observed for **1** that established the configuration of the tetracyclic core (side chain eliminated for clarity).

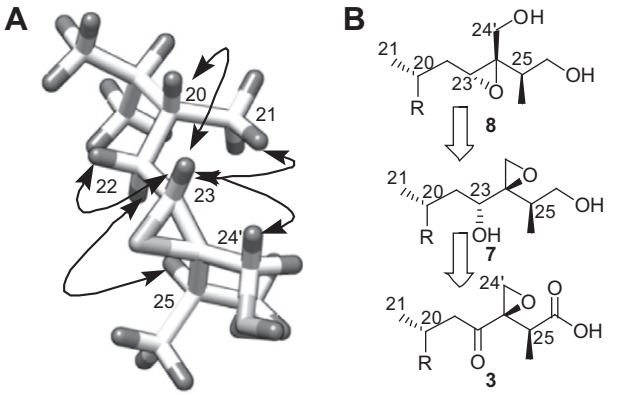

Figure 7. Analysis of the Payne rearrangement product **8**. (A) Configuration suggested by analyses of $^{3}J_{HH}$ values and NOE correlations that define a 20*R*, 23*R*, 24*R*, 25*R* configuration of **8**. (B) Relating the configuration of **8** to the natural product **3**.

rearrangement, the actual configuration of C-23 in the reduction product **7** would be irrelevant. Either C-23 epimer would be expected to undergo the Payne rearrangement, although producing spectroscopically distinct diastereomers of **8**. One diastereomer of **7** would produce the *cis*-epoxide, while the other would yield the *trans*-epoxide. It would not be necessary to know at the outset which C-23 epimer of **7** was the major reduction product or which was used in the Payne rearrangement. The key would be to relate the configuration of C-23 to C-20 in **8**, and be able to establish a *cis*- or *trans*-configuration for the epoxide at C-23 and C-24. Based on those two pieces of data, it should be possible to deduce the configuration of C-24 in **3**.

Preparation of the derivative **8**, which was needed to assign the configuration of C-24 in **3**, proceeded smoothly. A methanolic solution of **5** was reduced with an excess of $NaBH_4$ to generate **7** (3.1 mg; *Table* S4) after HPLC purification. Literature precedents suggest the reduction transition state should have the C_{24}–O bond perpendicular to the C=O bond, so that the σ^* orbital of the former can interact with the π^* orbital of the latter bond.[13,14] This conformation would produce the *anti* reduction product, although as mentioned above, the exact stereochemical outcome of the reduction is irrelevant at this point. Refluxing compound **7** with K_2CO_3 in distilled *i*-PrOH[15] yielded **8** after purification (**8**, 1.0 mg, Fig. 6). Subsequent 2D NMR analyses in $CDCl_3$ confirmed the identity of the product (Table S5). Unfortunately, the resonances for H_3-21 and H_3-27 were overlapped, which prevented the accurate assignment of key NOE correlations observed in this solvent. After screening several alternatives, MeOH-d_4 provided the best dispersion of the resonances for H_3-21 and H_3-27.

Detailed analyses of the 1D TOCSY and 1D DPFGSE NOE NMR spectra of **8** recorded in MeOH-d_4 secured the relative configurations of the stereogenic centers C-20, C-23, and C-24 (Fig. 7). An NOE correlation (Fig. S40) was observed between H-23 (δ_H 3.01) and H_2-24′ (δ_H 3.76 and δ_H 3.46) thus defining their *cis* relationship across the epoxide in **8** (Fig. 7A). Using the criteria outlined by Murata,[16] the configuration of H-23 (δ_H 3.01, dd; J = 7.5, 3.6 Hz) could then be related to H-20 (δ_H 1.65, m) as follows. A large coupling ($^{3}J_{H,H}$ = 8.5 Hz, Fig. S38) was observed between H-20 and H-22a (δ_H 1.22, dt; J = 14.5, 8.5 Hz), which defined an *anti* orientation between these two protons. An NOE correlation (Fig. S40) between H_3-21 (δ_H 1.07, d; J = 6.4 Hz) and H-23 then established C-21 and C-23 were *gauche* with respect to the C-20 and C-22 single bond. H-22a was then related to H-23 on the basis of a large $^{3}J_{H22a,H23}$ coupling observed ($^{3}J_{H,H}$ = 7.5 Hz; Fig. S38), which defined their *anti* orientation. Given these constraints, analyses of the viable conformations for the two possible diastereomers of **8** (23*R*, 24*R* and 23*S*, 24*S*) established *R*-configurations at all the stereogenic centers in the side chain of **8** (Fig. 7), and thus a 20*R*, 24*R*, 25*S*[17] configuration in the natural product **3** (Fig. 7B). The NOE correlation observed between H-23 and H_3-21 was the key to the assignment, as this would not be observed in the other diastereomer which must have these two groups are *anti* to each other, given the required *anti* orientations of H-23/H-22a and H-22a/H-20 defined by their large proton–proton coupling constants (Fig. S45).

During our initial screening, this extract potently inhibited the BACE1-mediated cleavage of amyloid precursor protein (APP) at our screening concentration of 50 μg/mL. Bioassay-guided fractionation traced this activity to **3**, which inhibited BACE1 with a modest IC_{50} value of 14.2 μM. Interestingly, **4** which lacks the terminal epoxide is not active in this assay, suggesting that the electrophilic epoxide in **3** may form a covalent linkage with BACE1. While **3** is the first example of a triterpene inhibitor of BACE1, two *ent*-kaurene-type diterpenoid inhibitors were previously reported from the perennial herb *Aralia cordata*.[18]

Compounds **1–3** are lanostane-type triterpenes[19] that are modified by the addition of a single carbon atom at C-24[20] and have the configuration of C-3 inverted.[21] The closest structural relative is carboxyacetylquercinic acid isolated from a Japanese fungus[22] of the same genus, *Daedalea dickisii*. Triterpenes are relatively common from this genus, constituting the bulk of the secondary metabolites reported,[8,23] thus our report is consistent

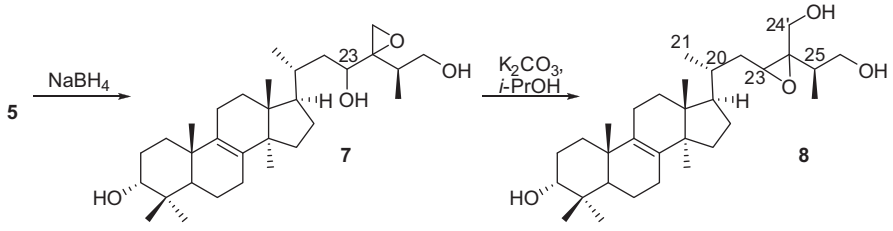

Figure 6. Derivatives of **3** prepared to deduce the configuration of C-24.

with other findings. The most unusual structural feature of this series of compounds is the terminal epoxide at C-24′ of **3**. Epoxidation at this position of the side chain always occurs as an internal epoxide,[24–26] and other than **3**, there are few other examples of a tetracyclic triterpene containing a terminal epoxide at this position.

A notable aspect of this work is the use of a Payne rearrangement. Originally reported in 1962,[11] Payne rearrangements underwent a renaissance in the last few decades due to the wide-spread use of Sharpless asymmetric epoxidations.[27] While α-epoxy ketone moieties, such as that found in **3**, occur in natural products,[28,29] there are few reliable methods to assign the configuration of these units in acyclic systems.[30,31] Thus, the approach demonstrated here may be of use to others.

2. Experimental section

2.1. General experimental procedures

Optical rotations were measured on a Jasco-DIP-700 polarimeter at the sodium line (589 nm). UV spectra were obtained on a Hewlett–Packard 8453 spectrophotometer. IR spectra were measured as a thin film on NaCl or CaF_2 plates using a Perkin–Elmer 1600 series FTIR. NMR spectra were acquired on a Varian Inova 500 MHz spectrometer operating at 500 or 125 MHz using the residual solvent signals as an internal reference (CD_3OD δ_H 3.30; δ_C 49.0, and $CDCl_3$ δ_H 7.26; δ_C 77.3). High-resolution mass spectrometric data were obtained on an Agilent MSD-TOF with ES or APC ionization in the positive mode. Gradient separations were performed on a Shimadzu HPLC system consisting of a LC-20AB solvent delivery module, a SPD-M20A photodiode array detector, a SCL-20A VP system controller, and an Alltech ELSD 800.

2.2. Biological material

The sporocarp designated 122899-SOLE-1 was collected on a tree located on the river banks of the 'RIO SOLE' in the community of Guaca, near David City, Chiriqui, Panama, on December 28, 1999. The sample was identified as a *Daedalea* sp. by G. Wong, UH Manoa Department of Botany. A voucher sample is maintained at the University of Hawai'i at Manoa.

2.3. Extraction and isolation

The field-collected fungal sample was extracted three times, each for 16 h, with a mixture of 70% MeOH, 20% EtOAc and 10% MTBE. Reversed-phase (C_8) chromatographic separation of the bulk extract, using increasing amounts of MeOH in water as the eluent (25–100%), resulted in four fractions (A–D) after TLC analyses. Fraction B (50% MeOH, 162.1 mg) was separated into four fractions (B1–B4) by RP-HPLC (Jupiter C_{18}; 250 × 10 mm, 300 Å), eluting with a linear gradient of 70–100% MeOH in water over 40 min (flow rate 3 mL/min). Final purification of fraction B4 (46.9 mg), using a linear gradient (25 min) of 82–85% MeCN in water, containing 0.1% formic acid, yielded **1** (t_R 18 min, 1.7 mg, 0.031% yield). RP-HPLC separation of fraction B3 (57.7 mg) on the Jupiter column, using a linear gradient (40 min) of 80–100% MeCN in 0.1% aq. formic acid, yielded **2** (t_R 34 min, 3.0 mg, 0.056% yield). Isocratic purification (65% MeCN) of fraction B2 resulted in **3** (t_R 29 min, 1.8 mg, 0.033% yield) and **4** (t_R 32 min, 2.4 mg, 0.045% yield).

2.4. Daedalol A (1)

White powder; $[\alpha]_D^{25}$ +20 (*c* 1.0, MeOH); UV (MeOH) λ_{max} ($\log\varepsilon$) 204 (3.40) nm; IR (MeOH) ν_{max} 3447, 1671, 1547, 1451, 1367 cm^{-1}; See Table 1 for tabulated NMR data; HR-ESI(+)-MS $[M+H]^+$ *m/z*: 485.3612 (calcd for $C_{31}H_{49}O_4^+$, 485.3631; Δ = −3.9 ppm).

2.5. Daedalol B (2)

White powder; $[\alpha]_D^{25}$ +56 (*c* 0.2, MeOH); UV (MeOH) λ_{max} ($\log\varepsilon$) 205 (8.34) nm; IR (MeOH) ν_{max} 3446, 1705, 1704, 1643, 1555, 1540, 1457, 1374, 1203, 899, 804, 754 cm^{-1}; See Table S1 for tabulated NMR data; HR-ESI(+)-MS $[M+H]^+$ *m/z*: 469.3686 (calcd for $C_{31}H_{49}O_3^+$, 469.3682; Δ = 0.9 ppm).

2.6. Daedalol C (3)

White powder; $[\alpha]_D^{25}$ +15 (*c* 0.2, MeOH); UV (MeOH) λ_{max} ($\log\varepsilon$) 206 (0.57) nm; IR (MeOH) ν_{max} 3391, 1712, 1642, 1585, 1450, 1405, 1315, 1262, 1091, 1025 cm^{-1}; See Table 2 for tabulated NMR data; HR-ESI(+)-MS $[M-C_3H_4O_4+H]^+$ *m/z*: 483.3500 (calcd for McLafferty rearrangement product $C_{31}H_{47}O_4^+$, 483.3474; Δ = 5.3 ppm).

2.7. Methylation of the crude extract

A portion of the crude extract (100 mg) was dissolved in 1.2 mL of toluene and 0.8 mL of MeOH. The resulting solution was treated with 100 μL of $TMSCHN_2$ (2 M in hexane), and stirred for 30 min until bromocresol green TLC analyses indicated the reaction was complete. After quenching with dilute acetic acid, the desired methyl esters were purified from the crude reaction residue by Si HPLC (Luna; 250 × 10 mm), using a linear gradient of 10–25% EtOAc in hexane over 40 min, to yield compounds **5** (t_R 26 min, 35.7 mg) and **6** (t_R 31 min, 30.2 mg).

2.8. Methyl daedalol A (5)

White powder; $[\alpha]_D^{25}$ +44 (*c* 0.1, $CHCl_3$); UV ($CHCl_3$) λ_{max} ($\log\varepsilon$) 241 (5.85) nm; IR (CCl_4) ν_{max} 1736, 1457, 1437, 1373, 1310, 1264, 1203, 1154 cm^{-1}; See Tables S2 and S3 for tabulated NMR data; HR-ESI(+)-MS $[M+H]^+$ *m/z*: 615.3884 (calcd for $C_{36}H_{55}O_8^+$, 615.3897, Δ = −2.1 ppm).

2.9. Reduction of 5

A 14.4 mg sample of **5** was dissolved in 5 mL of DCM and cooled in an ice bath. To this solution was added 760.3 mg of $NaBH_4$ in 1 mL of MeOH. The reaction was allowed to slowly warm to room temperature. After 5 h, the reaction was quenched, evaporated to dryness, and partitioned between diethyl ether and H_2O. Purification of the organic residue on a Luna silica analytical column, using a linear gradient of 5–50% EtOAc in hexane over 20 min, yielded 3.1 mg of **7** (24% yield).

2.10. Compound 7

Amorphous powder; $[\alpha]_D^{25}$ −6 (*c* 0.3, MeOH); UV (MeOH) λ_{max} ($\log\varepsilon$) 206 (4.60) nm; IR (MeOH) ν_{max} 3389, 1644, 791 cm^{-1}; See Table S4 for tabulated NMR data; HR-ESI(+)-MS $[M+Na]^+$ *m/z*: 511.3767 (calcd for $C_{31}H_{52}O_4Na^+$, 511.3763, Δ = 0.9 ppm).

2.11. Payne rearrangement

A sample of **7** (2.1 mg) was refluxed along with 427.9 mg of K_2CO_3 in 4 mL of *i*-PrOH for 3 h. The residue from the organic partition of this reaction mixture was then separated by RP-HPLC, using a linear gradient of 40–80% EtOAc in hexane over 30 min, to yield the major product **8** (t_R 29 min, 1.1 mg, 36% yield).

2.12. Compound 8

White powder; $[\alpha]_D^{25}$ +2 (*c* 1.0, $CHCl_3$); UV (MeOH) λ_{max} (logε) 207 (4.92) nm; IR ($CHCl_3$) ν_{max} 3425, 1643 cm^{-1}; See Table S5 for tabulated NMR data; HR-ESI(+)-MS $[M+Na]^+$ *m/z*: 511.3791 (calcd for $C_{31}H_{52}O_4Na^+$; 511.3763, Δ = 5.6 ppm).

2.13. BACE1 assay

The proteolytic cleavage of amyloid precursor protein was assayed as described by Naqvi.[6,32] Test compounds were dissolved in DMSO at the desired concentrations, and incubated in 96 well plates with the enzyme for 16 h in triplicate. A DMSO control (1.5 μL) and an inhibitor standard were also tested in triplicate. The chemiluminescence signal was read using a Fluorostar Optima spectrophotometer. Data were analyzed using GraphPad Prism. BACE1 activity was calculated as a percent of the positive control using a nonlinear regression analysis function that corresponded to a best one-fit model.

Acknowledgments

This work was funded by grants from the Victoria S. and Bradley L. Geist Foundation (20070461), the Alzheimer's Association (NIRG-08-90880), the Alzheimer's Drug Discovery Foundation (281204), and the National Institute of Aging (5R21AG032405). Funds for the upgrades of the NMR instrumentation were provided by the CRIF program of the National Science Foundation (CH E9974921) and the Elsa Pardee Foundation. The purchase of the LC-MS-TOF was funded by grant W911NF-04-1-0344 from the Department of Defense.

Supplementary data

Supplementary data (copies of the ^1H, ^{13}C and 2DNMR spectroscopic data for all new compounds associated with this article, along with 1D TOCSY and 1D NOE spectra for **8**) associated with this article can be found, in the online version, at doi:10.1016/j.bmc.2011.09.029.

References and notes

1. Citron, M. *Nat. Rev. Drug Disc.* **2010**, *9*, 387.
2. Hardy, J. *J. Alzheimer's Dis.* **2006**, *9*, 151.
3. Hardy, J.; Selkoe, D. J. *Science* **2002**, *297*, 353.
4. Hardy, J. A.; Higgins, G. A. *Science* **1992**, *256*, 184.
5. Eglen, R. M. *Assay Drug Dev. Technol.* **2002**, *1*, 97.
6. Naqvi, T. *J. Biomol. Screen.* **2004**, *9*, 398.
7. Chairul; Tokuyama, T.; Nishizawa, M.; Shiro, M.; Tokuda, H.; Hayashi, Y. *Phytochemistry* **1990**, *29*, 923.
8. Rösecke, J.; König, W. A. *Phytochemistry* **2000**, *54*, 757.
9. Kühnel, E.; Laffan, D. D. P.; Lloyd-Jones, G. C.; Martínez del Campo, T.; Shepperson, I. R.; Slaughter, J. L. *Angew. Chem., Int. Ed.* **2007**, *46*, 7075.
10. Presser, A.; Hufner, A. *Monatsh. Chem.* **2004**, *135*, 1015.
11. Payne, G. B. *J. Org. Chem.* **1962**, *27*, 3819.
12. Hanson, R. M. *Org. React.* **2002**, *60*, 1.
13. Chérest, M.; Felkin, H.; Prudent, N. *Tetrahedron Lett.* **1968**, *9*, 2199.
14. Anh, N.; Eisenstein, O. *Nouv. J. Chem.* **1977**, 61.
15. Koizumi, N.; Ishiguro, M.; Yasuda, M.; Ikekawa, N. *J. Chem. Soc., Perkin Trans. I* **1983**, *7*, 1401.
16. Matsumori, N.; Kaneno, D.; Murata, M.; Nakamura, H.; Tachibana, K. *J. Org. Chem.* **1999**, *64*, 866.
17. The stereochemical description of C-25 differs in **3** (25*S*) and **8** (25*R*), as a consequence of the increased priority of C-26 in **3** according to the Cahn–Ingold–Prelog rules.
18. Jung, H. A.; Lee, E. J.; Kim, J. S.; Kang, S. S.; Lee, J. H.; Min, B. S.; Choi, J. S. *Arch. Pharm. Res.* **2009**, *32*, 1399.
19. Windaus, A.; Tschesche, R. *Z. Physiol. Chem.* **1930**, *190*, 51.
20. Dewick, P. M. *Medicinal Natural Products: A Biosynthetic Approach*; Wiley, 2002.
21. Pal, R.; Kulshreshtha, D. K.; Rastogi, R. P. *Phytochemistry* **1975**, *14*, 2253.
22. Yoshikawa, K.; Kouso, K.; Takahashi, J.; Matsuda, A.; Okazoe, M.; Umeyama, A.; Arihara, S. *J. Nat. Prod.* **2005**, *68*, 911.
23. Kawagishi, H.; Li, H.; Tanno, O.; Inoue, S.; Ikeda, S.; Ohnishi-Kameyama, M.; Nagata, T. *Phytochemistry* **1997**, *46*, 959.
24. Kenji, G. M.; Nakajima, S.; Baba, N.; Iwasa, J. *Chem. Express* **1991**, *6*, 233.
25. Su, B.-N.; Chai, H.; Mi, Q.; Riswan, S.; Kardono, L. B. S.; Afriastini, J. J.; Santarsiero, B. D.; Mesecar, A. D.; Farnsworth, N. R.; Cordell, G. A.; Swanson, S. M.; Kinghorn, A. D. *Bioorg. Med. Chem.* **2006**, *14*, 960.
26. Liu, H.; Heilmann, J.; Rali, T.; Sticher, O. *J. Nat. Prod.* **2001**, *64*, 159.
27. Katsuki, T.; Sharpless, K. B. *J. Am. Chem. Soc.* **1980**, *102*, 5974.
28. Choudhary, M. I.; Ismail, M.; Shaari, K.; Abbaskhan, A.; Sattar, S. A.; Lajis, N. H.; Atta-ur-Rahman *J. Nat. Prod.* **2010**, *73*, 541.
29. Kwan, J. C.; Teplitski, M.; Gunasekera, S. P.; Paul, V. J.; Luesch, H. *J. Nat. Prod.* **2010**, *73*, 463.
30. Chevallier, C.; Bugni, T. S.; Feng, X.; Harper, M. K.; Orendt, A. M.; Ireland, C. M. *J. Org. Chem.* **2006**, *71*, 2510.
31. Djerassi, C.; Klyne, W.; Norin, T.; Ohloff, G.; Klein, E. *Tetrahedron* **1965**, *21*, 163.
32. Millán-Aguiñaga, N.; Soria-Mercado, I. E.; Williams, P. *Tetrahedron Lett.* **2010**, *51*, 751.